Numerical Simulation of Fire Resistance of Austenitic 1.4103 Stainless Steel Beams in Different Sections

Andre L. Zanoni[1], Paulo A. G. Piloto[2], Luiz M. R. Mesquita[3], Diego R. Rossetto[4]

[1,4]Federal Technological University of Paraná (UTFPR), Campus Pato Branco, 85503-390, Brazil.
e-mail: [1]andrezanoni@alunos.utfpr.edu.br, [4]diegorossetto@utfpr.edu.br
[2,3]Polytechnic Institute of Bragança (IPB), Campus Santa Apolónia, 5300-253, Portugal.
e-mails: [2]ppiloto@ipb.pt , [3]lmesquita@ipb.pt

Abstract. Stainless steel structures are increasingly used in civil engineering due to their mechanical strength and corrosion resistance. However, under fire conditions, their performance may degrade significantly. This study investigates the fire resistance of austenitic 1.4301 stainless steel beams using finite element simulations in ANSYS. A parametric analysis was performed considering seven different rectangular hollow sections, exposed to ISO 834 fire conditions on and subjected to bending. Geometrically and materially nonlinear analysis (GMNIA) was applied to evaluate thermal and mechanical responses. The results indicate that section geometry, especially thickness and width, significantly influences both temperature distribution and structural performance during fire exposure. Beams with greater thickness exhibited lower internal temperatures and improved fire resistance times. These findings support the optimization of stainless steel beam designs for enhanced fire safety.

Keywords: fire resistance; stainless steel; finite element analysis; thermo-mechanical behavior; beam sections.

1. Introduction

Stainless steel, introduced in the early 20th century, is known for its corrosion resistance, strength, and aesthetic appeal [6]. Despite higher initial costs, its use in structures has increased, especially the austenitic class [7, 8, 9]. Rectangular Hollow Section (RHS) beams are particularly valued for their structural performance [10, 11, 12].

However, its behavior at elevated temperatures must be thoroughly studied, particularly under fire exposure, which can significantly affect its mechanical properties and structural integrity.

Fires remain a critical threat to urban environments, with significant impacts on life and infrastructure [1, 2]. To ensure structural safety, it is essential to understand how materials behave under elevated temperatures [3, 4]. In Europe, the Structural Eurocodes provide guidelines for assessing fire resistance, with Part 1-2 addressing material-specific behavior under fire [5].

This study applies the Finite Element Method (FEM) via ANSYS to simulate the fire behavior of 1.4301 stainless steel beams. Previous research has validated similar simulations with good agreement to experimental data [13, 14, 15]. A parametric approach is used to analyze how variations in beam geometry affect thermal behavior and fire resistance, contributing to safer and more efficient structural designs.

2. Materials and Methods

This study focuses on the thermo-mechanical behavior of austenitic stainless steel beams (grade 1.4301) under fire conditions. Mechanical properties such as yield and ultimate strength were defined according to EN 1993-1-4 [16], considering both cold-formed and hot-rolled profiles with nominal thicknesses up to 12 mm. Stress-strain relationships were derived from Eurocode 3 [5] using temperature-dependent Ramberg-Osgood equations, with adaptations for corner regions based on Ashraf et al. [17].

Thermal properties, including thermal conductivity, specific heat, and emissivity, were modeled according to EN 1993-1-2 [5], using temperature-dependent functions. Fire exposure followed the ISO 834 standard curve [18]. Seven

RHS cross-sections were analyzed (e.g., 100×50×5 mm to 300×200×8 mm). Each beam had a total length of 3750 mm and an effective fire exposure zone of 3160 mm. Loads were applied symmetrically at a distance of 1200 mm from each support. The geometry and fire exposure region adopted for the simulations are shown in in Figure 1.

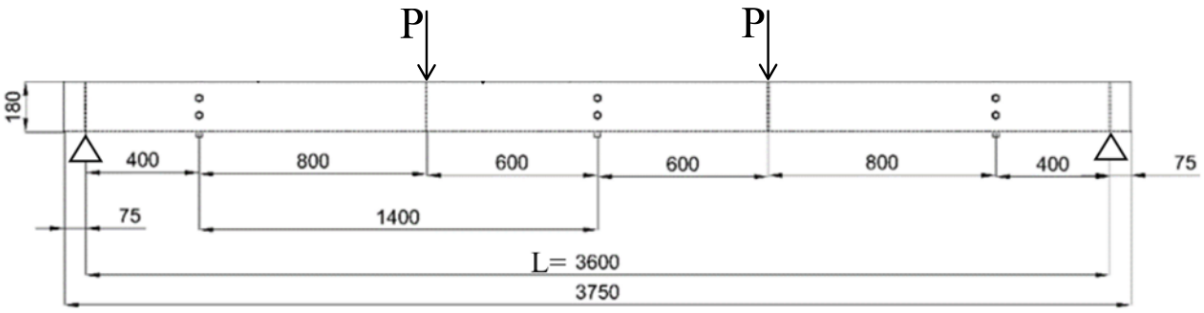

Figure 1. Beam geometry and fire exposure region (*adapted from* [19]).

Slenderness was evaluated using EN 1993-1-2 and EN 1993-1-5 [20], ensuring sections remained within the valid range for the applied method. Seven RHS cross-sections were analyzed, varying in height, width, and thickness. Their dimensions and shapes are presented in Table 1.

Table 1 – Cross-sections analyzed in the parametric study (*adapted from* [21]).

Geometry	Section	h [mm]	b [mm]	t [mm]	r [mm]
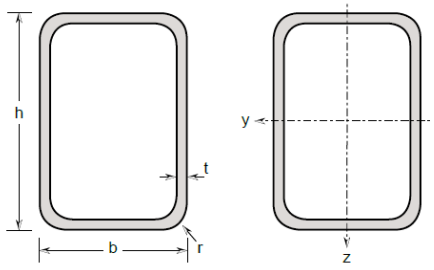	100x50x5	100	50	5	10
	150x80x4	150	80	5	10
	150x100x5	150	100	5	10
	180x100x5	180	100	5	10
	200x100x5	200	100	5	10
	300x200x5	300	200	5	10
	300x200x8	300	200	8	20

Numerical simulations were performed in ANSYS 2024, using SHELL131 elements for thermal analysis and SHELL181 for static and thermo-mechanical stages. The analysis sequence comprised three steps:

i. **Static analysis (20 °C):** to define the maximum load-bearing capacity per section, using large displacement nonlinear settings.
ii. **Thermal analysis**: to simulate temperature distribution over time with convective and radiative heat transfer. Boundary conditions were applied on three sides of the beam over the fire-exposed region.
iii. **Thermo-mechanical analysis**: to assess fire resistance under sustained load levels (0.2, 0.4, and 0.6 of maximum static load), integrating the previous results. Failure criteria were based on displacement thresholds and convergence behavior [22].

Material data and stress-strain curves were generated using Excel, and all models considered geometrical and material nonlinearities with initial imperfections (GMNIA). Mesh refinement followed convergence criteria and varied with section dimensions.

3. Results and Discussion

The study includes results from the static, thermal and thermomechanical analyses. In the static analysis, the val-

ues of the maximum force supported by each cross-section are presented. Analysing the strength of each section Figure 2.

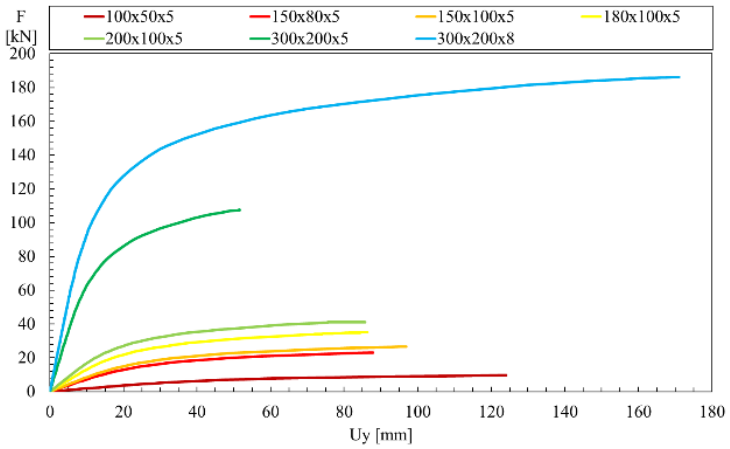

Figure 2 – Comparison of the strength at room temperature of the cross sections for the austenitic 1.4301 stainless steel.

The graphs show a section resistance as the width, height or thickness is varied (Figure 6). When comparing sections of the same height and varying their width, as in the case of the RHS 150x80x5 and RHS 150x100x5 sections (Figure 6), there is a slight increase in the resistance of the sections. When the thickness was varied, as in the case of the 300x200x5 and 300x200x8 cross-sections, there was a large increase in both the maximum force supported and the maximum displacement due to the better distribution of the force over the beam [23].

When the section height was varied between the 150x100x5 and 180x100x5 sections, it was found that the maximum force supported by the cross-section showed a significant jump, varying by around 30 per cent more. On the other hand, the maximum displacement obtained decreased by 10 per cent These results were obtained from the data in Table 2, which shows the maximum force supported by each section and its maximum displacement achieved by the convergence of the software [15].

Table 2 – Maximum force and displacement at room temperature supported by each beam cross-section.

Section	**Maximum Force NUM [kN]**	**Displacement axis-Y [mm]**
100x50x5	9.71	124.03
150x80x5	23.18	87.86
150x100x5	26.64	96.81
180x100x5	35.04	86.29
200x100x5	41.20	85.73
300x200x5	107.44	51.57
300x200x8	186.14	171.03

The temperature as a function of time was obtained for four points (T1 to T4) distributed along the height of the beam cross-section, as illustrated in Figure 3. The cross-section was exposed to fire on three sides—bottom and vertical webs—according to standard ISO 834 fire conditions. These data allowed the analysis of thermal variation among different geometries.

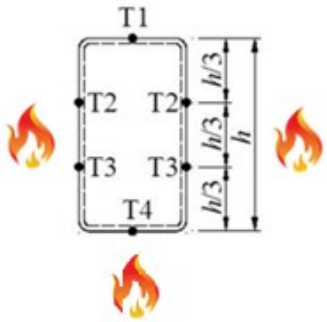

Figure 3 – Temperature measurement points in the cross-section exposed to fire on three sides. (adapted from [19]).

Increasing one of the beam's dimensions results in greater mechanical resistance. For thermal analyses, the thermal properties can be observed in Figure 4.

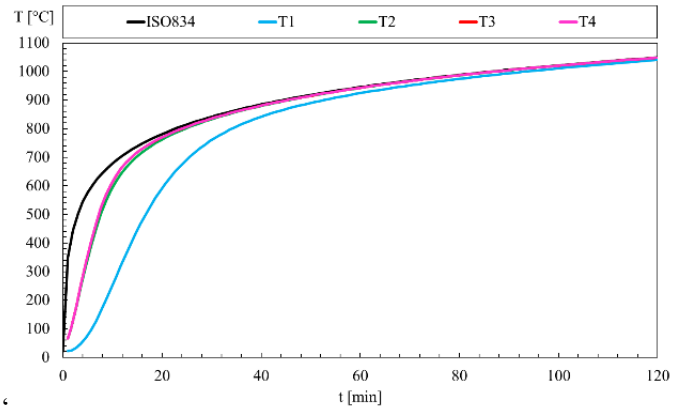

Figure 4 – Thermal data section RHS180x100x5 for austenitic stainless steel.

Between different sections, there is a significant variation in the temperature distribution among the section. When considering the three geometric parameters (height, width and thickness), as the height of the section increases, the temperatures at points T1, T2, T3 and T4 remain practically unchanged between the different sections Figure 5, illustrates the comparison between the RHS 200x100x5 and RHS 180x100x5 cross-sections.

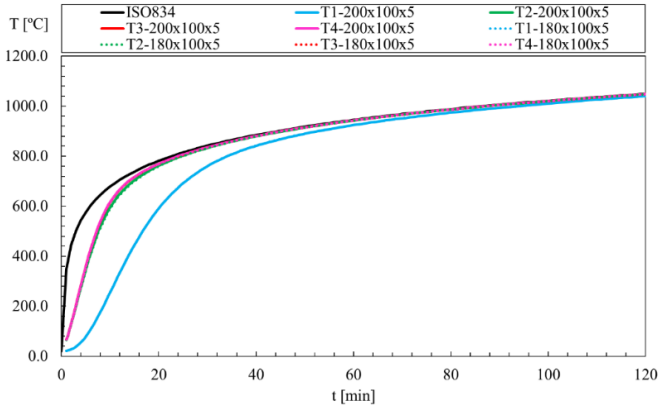

Figure 5 – Comparison of thermal capture points T1, T2, T3 and T4 between sections RHS 200x100x5 and RHS 180x100x5.

Keeping the height and thickness of the section constant and varying the width, there is a significant difference in temperature at point T1, while points T2, T3 and T4 show no variation, as illustrated in Figure 6, which compares the RHS 150x100x5 and RHS 150x80x5 sections.

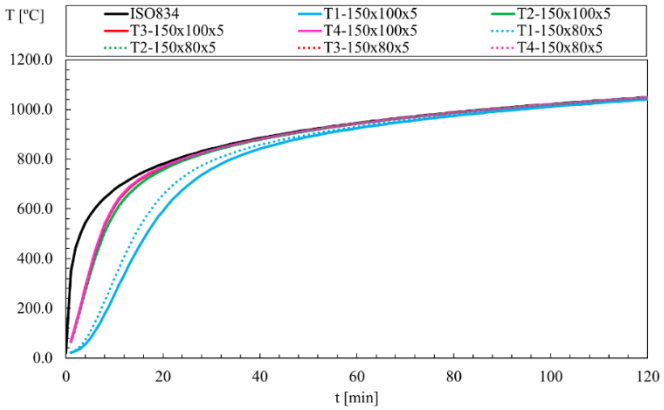

Figure 6 – Comparison of thermal capture points T1, T2, T3 and T4 between sections RHS 150x100x5 and RHS 150x80x5.

When using different thicknesses, keeping the height and width constant, all the temperature points show lower values in the thicker sections. This behaviour can be seen in Figure 7, which compares the RHS 300x200x5 and RHS 300x200x8 sections.

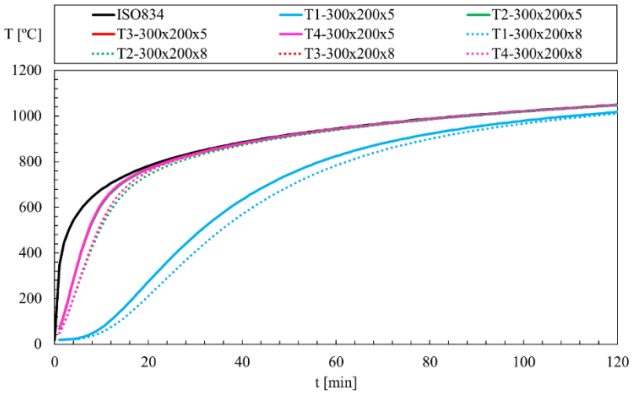

Figure 7 – Comparison of thermal capture points T1, T2, T3 and T4 between sections RHS 150x100x5 and RHS 150x80x5.

It can therefore be seen that the width and thickness of the section influence the temperature distribution in the beam more significantly than the height. This is because the temperature is distributed over a larger surface [24].

For the parametric thermo-mechanical analyses, the maximum loads obtained in the static simulations were applied and distributed according to the number of nodes in each section, considering loads of 0.2, 0.4 and 0.6 of the maximum loads. The aim was to determine the final time and critical temperature at which the beam maintains its structural integrity under this stress, using the stopping criteria (Equations 4 and 5) or terminating the simulation if the software failed to converge.

Table 3, shows the supported time for each section depending on load.

Table 3 – Final time and maximum temperature of thermomechanical simulations.

Section	Load Level	D_{limit} [mm]	$(dD/dt)_{limit}$ [mm/min]	Criteria 1	Criteria 2	t_{fi} [min]	T_{max} [ºC]
100x50x5	0.2	324	14.4	-	-	46.50	904
	0.4			-	23.00	25.23	808
	0.6			-	-	11.00	641
150x80x5	0.2	216	9.6	-	51.83	52.67	923
	0.4			-	-	25.00	806
	0.6			-	-	14.50	710
150x100x5	0.2	216	9.6	-	52.17	52.83	923
	0.4			-	-	26.55	817
	0.6			-	14.00	14.67	713
180x100x5	0.2	180	8	-	51.67	55.00	929
	0.4			-	26.83	27.67	823
	0.6			-	13.67	15.50	724
200x100x5	0.2	162	7.2	-	51.33	56.50	933
	0.4			-	26.50	28.17	825
	0.6			-	13.33	16.17	732
300x200x5	0.2	108	4.8	-	59.67	63.83	952
	0.4			-	27.33	37.00	868
	0.6			-	12.67	19.50	765
300x200x8	0.2	108	4.8	-	54.83	66.17	926
	0.4			-	14.00	31.67	723
	0.6			-	9.33	18.17	500

4. Conclusion

The parametric analyses indicated that, among the geometric factors evaluated, increases in thickness and width led to significant variations in the temperature distribution over time along the beam. This behavior is attributed to thermal conduction phenomena, as a greater material volume impedes heat propagation, resulting in a slower heating process. In the static analyses, an enhancement in resistance at 20 °C was observed with the increase in height, width, and thickness of the cross-sections. A similar trend was identified in the thermo-mechanical analyses, albeit to a lesser extent. This reduced sensitivity is explained by the simulations being based on the maximum load-bearing capacity at room temperature, which limits the ability to discern the influence of geometric variations under the assessed conditions.

Authorship statement. The authors hereby confirm that they are the sole liable persons responsible for the authorship of this work, and that all material that has been herein included as part of the present paper is either the property (and authorship) of the authors, or has the permission of the owners to be included here.

References

[1] Reis, A. da S. (2011). Determinação de cenários de incêndio em edifícios. *[Dissertação de Mestrado]*. Universidade de Aveiro, Departamento de Engenharia Civil.
[2] Figueiredo, P. J. F. (2018). Segurança contra Incêndios em Edifícios de Centros Urbanos Antigos – Antigo Orfeão e o Centro Histórico de Viseu. *[Dissertação de Mestrado]*. Departamento de Engenharia Civil, Instituto Superior de Engenharia de Coimbra.
[3] Del Prete, I., Cefarelli, G., & Nigro, E. (2016). Application of criteria for selecting fire scenarios for structures within fire safety engineering approach. *Journal of Building Engineering, 8*, 208-217. https://doi.org/10.1016/j.jobe.2016.10.010.
[4] Landesmann, A., & Mouço, D. L. (2007). Análise estrutural de um edifício de aço sob condições de incêndio. *Revista Escola de Minas, Ouro Preto, 60(2)*, 285-294. https://doi.org/10.1590/S0370-44672007000200011.

[5] CEN. (2023). FprEN 1993-1-2: Eurocode 3 - Design of steel structures - Part 1-2: Structural fire design. *European Committee for Standardization*.
[6] Gardner, L. (2005). The use of stainless steel in structures. *Progress in Structural Engineering and Materials, 7(2)*, 45-55. https://doi.org/10.1002/pse.190.
[7] Gardner, L., & Theofanous, M. (2008). Discrete and continuous treatment of local buckling in stainless steel elements. *Journal of Constructional Steel Research, 64(11)*, 1207-1216. http://dx.doi.org/10.1016/j.jcsr.2008.07.003.
[8] Arrais, F., Lopes, N., & Real, P. V. (2021). Resistência ao fogo de vigas-coluna com seções elíticas ocas esbeltas em aço inoxidável. *7as Jornadas de Segurança aos Incêndios Urbanos, 2as Jornadas de Proteção Civil*, 214-222. ISBN: 978-989-54814-9-1.
[9] Wu, M., Fan, S., Han, Y., Liang, D., & Xu, Q. (2023). Fire-resistant design of stainless steel-concrete composite beam considering slip of stud connector. *Thin-Walled Structures, 186*, 110713. https://doi.org/10.1016/j.tws.2023.110713.
[10] Camacho, J. S. (2013). Estudo das vigas: flexão normal simples. *Faculdade de Engenharia de Ilha Solteira, Departamento De Engenharia Civil*.
[11] Chiew, S. P., Jin, Y. F., & Lee, C. K. (2016). Residual stress distribution of roller bending of steel rectangular structural hollow sections. *Journal of Constructional Steel Research, 119*, 85-97. http://dx.doi.org/10.1016/j.jcsr.2015.12.016.
[12] Vitali, D. (2024). Desenvolvimento de planilha de cálculo para definição de vigas metálicas de frigoríficos. *[Trabalho de Conclusão de Curso]*. Departamento de Engenharia Mecânica, Universidade de Passo Fundo.
[13] Lopes, N., Arrais, F., Vila Real, P., Alves, M., Mesquita, L., Piloto, P., & Pinho da Cruz, J. (2024). Fire resistance of austenitic stainless steel beams with rectangular hollow sections. *Fire and Materials, 48(1)*, 79-92. https://doi.org/10.1002/fam.3167.
[14] Real, P. V., Lopes, N., da Silva, L. S., & Franssen, J. M. (2008). Lateral–torsional buckling of stainless steel I-beams in case of fire. *Journal of Constructional Steel Research, 64(11)*, 1302-1309. https://doi.org/10.1016/j.jcsr.2008.04.013.
[15] Fan, S., Du, L., Li, S., Zhang, L., & Shi, K. (2019). Fire-resistance of RHS stainless steel beams with three faces exposed to fire. *Journal of Constructional Steel Research, 152*, 284-295. https://doi.org/10.1016/j.jcsr.2018.04.022.
[16] CEN. (2006). EN 1993-1-4: Eurocode 3 - Design of steel structures - Part 1-4: General rules - Supplementary rules for stainless steels. *European Committee for Standardization*.
[17] Ashraf, M., Gardner, L., & Nethercot, D. A. (2005). Strength enhancement of the corner regions of stainless steel cross-sections. *Journal of Constructional Steel Research, 61(1)*, 37-52. https://doi.org/10.1016/j.jcsr.2004.06.001.
[18] CEN. (2002). EN 1991-1-2: Eurocode 1 - Actions on structures - Part 1-2: General actions - Actions on structures exposed to fire. *European Committee for Standardization*.
[19] Fan, S., He, B., Xia, X., Gui, H., & Liu, M. (2016). Fire resistance of stainless steel beams with rectangular hollow section: Experimental investigation. *Fire safety journal, 81*, 17-31. http://dx.doi.org/10.1016/j.firesaf.2016.01.013.
[20] CEN. (2021). prEN 1993-1-5: Eurocode 3 - Design of steel structures - Part 1-5: Plated structural elements. *European Committee for Standardization*.
[21] Millstok Stainless. (2015). *Stainless Steel Sections Catalog*. Millstock Stainless Limited.
[22] Gardner, L., & Baddoo, N. R. (2006). Fire testing and design of stainless steel structures. Journal of Constructional Steel Research, 62(6), 532-543. doi:10.1016/j.jcsr.2005.09.009.
[23] Abdelrahman, A. A., Mohamed, N. A., & Eltaher, M. A. (2022). Static bending of perforated nanobeams including surface energy and microstructure effects. *Engineering with Computers, 38 (Suppl1)*, 415-435. https://doi.org/10.1007/s00366-020-01149-x.
[24] Abdulack, S. A. (2024). Transferência de calor em geometria cilíndrica: uma abordagem interdisciplinar para um problema real. *Revista Brasileira de Ensino de Física, 46*, e20240258. https://doi.org/10.1590/1806-9126-RBEF-2024-0258.